Functional Materials 16, No.2 (2009) © 2009 — STC "Institute for Single Crystals"

Surface morphology and structure of nanocrystalline diamond films deposited in $CH_4/H_2/Ar$ glow discharge plasma

I.I.Vyrovets, V.I.Gritsyna, S.F.Dudnik, O.A.Opalev, E.N.Reshetnyak, V.E.Strel'nitskiy

National Science Center "Kharkiv Institute of Physics and Engineering",
National Academy of Sciences of Ukraine,
1 Akademicheskaya St., 61108 Kharkiv, Ukraine

Received January 21, 2009

Diamond films of up to 12 μm thickness have been deposited onto single crystal silicon substrates by CVD method in $CH_4/H_2/Ar$ glow discharge plasma stabilized by magnetic field. X-ray diffraction analysis and atomic force microscopy have shown the films consist of about 1 μm in diameter conglomerates of 30–40 nm average size diamond nanocrystals. The conglomerate size increases by a factor of 2 as the film thickness grows from 1.7 up to 11.7 μm. At the same time, the nanocrystallite size remains essentially unchanged. In the diamond films, texture, compressive residual stresses and high concentration of crystal structure defects have been revealed.

Алмазные пленки толщиной до 12 мкм получены на подложках из монокристаллического кремния методом газофазного осаждения в $CH_4/H_2/Ar$ плазме тлеющего разряда, стабилизированного магнитным полем. Методами рентгеноструктурного анализа и атомно-силовой микроскопии установлено, что пленки состоят из конгломератов диаметром ~1 мкм, образованных нанокристаллами алмаза со средним размером 30–40 нм. С ростом толщины пленки от 1,7 до 11,7 мкм размер конгломератов увеличивается в 2 раза. При этом размер нанокристаллов практически не меняется. В пленках выявлены текстура, остаточные напряжения сжатия и высокое содержание дефектов кристаллического строения.

Recently, the materials in nano-crystalline state attract a great attention of researchers. These materials possess a number of unique properties as compared to single- and micro-crystalline ones, that extends both the application field and effectiveness thereof [1, 2]. In this respect, the diamond coatings are not an exception. One of the ways to achieve the grain refinement down to nano-size in the diamond films prepared by CVD is partial or full hydrogen substitution in the CH_4/H_2 gas mixture with argon. Thus, the deposition process is followed by an intense secondary nucleation hindering the diamond crystallite growth and holding their nano-sizes even at a significant (micrometers and tens of micrometers) film thickness. As a result, the films show a low roughness, high homogeneity of mechanical, thermo-physical and other properties being of importance for various film applications in tribology, optics, in manufacturing of planar non-heated cathodes, electronic emission devices, acoustic-electronic systems, etc. [3]. Nowadays, the microwave discharge is most often used for the working gas activation, but the equipment necessary for the process is expensive enough and complicated. The synthesis method can be substantially simplified if the magnetic field stabilized glow discharge is used to excite the gas mixture [4–6]. It was found that in such discharge type, the transition from coarse-crystalline to micro- and further to

nano-crystalline diamond coatings is realized at 20–40 % Ar concentrations in the gas mixture, that being substantially lower than the typical Ar contents in microwave discharge being at least 80 % [7, 8]. However, the peculiarities of structure and properties for such coatings are still not studied enough. The purpose of this work is to study the surface morphology, structure, and stress state in nano-crystalline diamond films prepared in $CH_4/H_2/Ar$ glow discharge plasma.

The diamond films of 1.7 to 11.7 μm thickness were deposited in the glow discharge in the $CH_4/H_2/Ar$ atmosphere stabilized by magnetic field onto the substrates of polished single-crystalline silicon with [111] orientation. Before deposition, the substrate was "sown" by mechanical indenting the ultra-disperse diamond (UDD) particles of 3 to 5 nm into its surface. According to microscopy data, such a preparation of the silicon surface provides the initial density of diamond nucleation up to $5 \cdot 10^8$ cm^{-2} [5]. Before the sowing, a part of the substrates were cleaned from the surface oxide layer using abrasive sandpaper and diamond paste. The gas mixture composition and pressure were selected both to provide the stable process of nano-structured film formation and to exclude glow discharge combustion failure due to micro-arc discharges on the cathode surface. The mixture pressure was $(1.1–1.2) \cdot 10^4$ Pa at CH_4 concentration of 0.8 to 1.0 % and Ar one of 40 %. The substrate temperature was kept at 890–920°C. The deposition rate was ~ 0.5 μm/h. The film effective thickness was determined from the deposited carbon amount using the gravimetric method. The diamond surface morphology was studied using a NT-206 atomic-force microscope.

The X-ray examinations including the analysis of phase composition, texture, substructure, and the residual stress evaluation in the films were carried out using a DRON-3 instrument in the copper anode filtered radiation. The diffraction patterns for the phase analysis were obtained by $\theta–2\theta$ scanning with Bragg-Brentano focusing in the 2θ angle range from 20 to 80 degrees using the continuous automatic recording onto chart strip. To study the film substructure and stress state, the diamond (111), (220), (311), (331) reflections were measured by point-wise intensity registration with $\Delta(2\theta)$ scan step of 0.02 to 0.1° and the 10–20 s pulse accumulation duration for a point (depending on diffraction maxima intensity and width). After preliminary treatment of diffraction patterns and doublet separation, the diffraction lines were approximated by Cauchy function. The coherence lengths (CL) in the diamond films were estimated using the Selyakov-Scherrer relation using the broadening of (220) reflection taking into account the line instrumental broadening of the standard and Scherrer constant. The residual stress in the coatings were analyzed by $\sin^2\psi$ method measuring the interplanar spaces during repeated oblique scans of (331) reflection positioned in the accuracy area of diffraction angles.

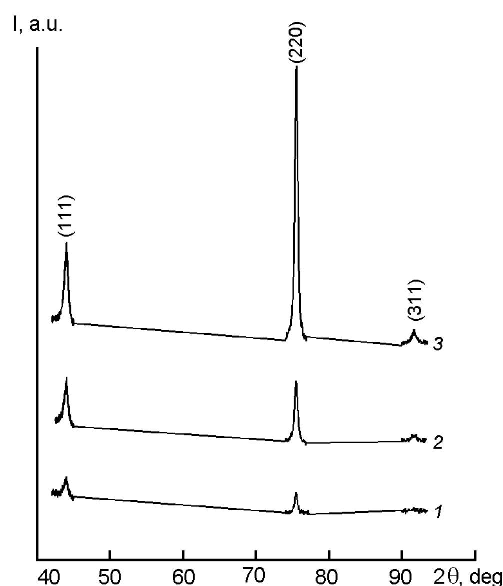

Fig. 1. Some parts of the diffraction patterns for diamond films of different thickness, μm: *1* — 1.7, *2* —4.6, *3* —9.8 01 (Cu-Kα radiation).

According to X-ray phase analysis data, all the coatings under study show the diffraction lines belonging to the only polycrystalline diamond phase (Fm3m space group of cubic syngony). As the film thickness grows, the line intensities increase (Fig. 1). However, the line intensity ratios differ substantially from the values typical of the powder samples with chaotic crystallite orientation, where the most intense line is (111). The most intense line observed in the film diffraction patterns corresponds to (220) reflection.That is connected with presence of texture in the films with the crystallite preferential <110> orientation along the normal to the substrate surface. It has been established that as the film thickness grows, the texture perfection increases. This is indicated by (220) line amplification

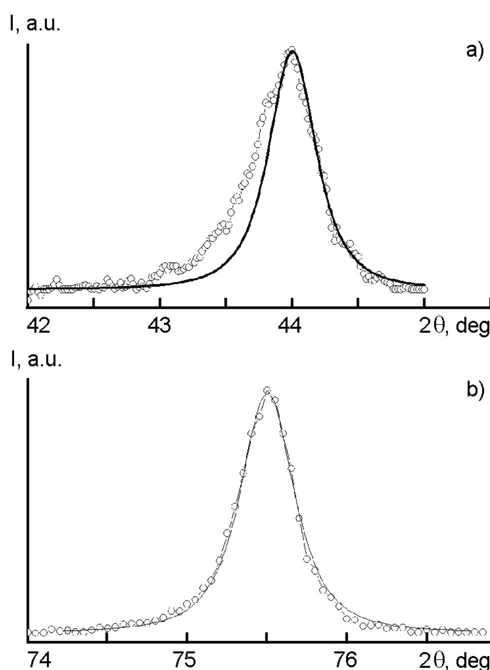

Fig. 2. Some parts of diffraction patterns for the sample of 9.8 μm thickness after the preliminary processing and Cauchy approximation. Reflections: (111) (a) and (220) (b).

in comparison with other reflections. Thus, the intensity ratios of (111), (220), and (311) lines for the sample of 1.7 μm thickness are 60:100:37, respectively, while for 11.7 μm thick sample, it is 22:100:4. The (220) reflection rocking curve width decreases from 19 to 15 degrees as the thickness grows.

The analysis of true physical broadening for different diffraction lines has shown that the (220) line is narrower than (111) one in all diffraction patterns. Thus, the line broadening is caused not only by the dispersity of the coherence areas and the elastic micro-strains in the films, i.e. not only by the dislocation defects of crystal structure. One of the causes of such abnormal broadening may be the presence of packing defects, which are formed in {111} planes of the diamond structure. It is known that the packing defects may result not only in the line broadening but also in their asymmetry and displacements which values depend on the interference indices [9, 10]. In Fig. 2, the parts of the diffraction pattern for a 9.8 μm thick sample are shown. The (111) and (220) diffraction lines are presented after the preliminary treatment and Cauchy approximation. It is seen that the experimental points for (220) line

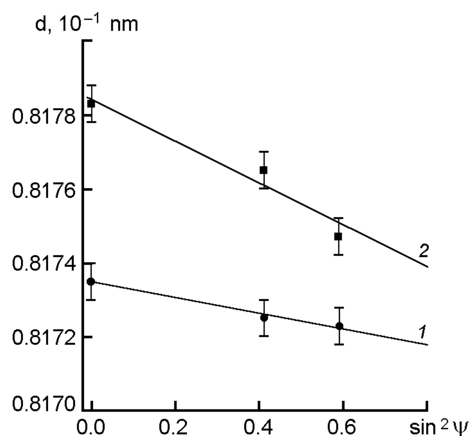

Fig. 3. $\mathrm{Sin}^2\psi$ plots for diamond films constructed using the oblique scanning results of (331) reflection. Film thickness, μm: 9.7 (*1*), 11.7 (*2*).

are well described by the symmetric Cauchy function, while the (111) line is rather asymmetric. Such the asymmetry of (111) line at the small-angle side is typical of all the samples studied, the asymmetry increasing as the thickness decreases. Moreover, the diamond crystal lattice constants calculated from the positions of different diffraction lines are different. This difference reaches 0.3 % and indicates the (220) line displacement to the large-angle side relative to the (311) line, that is typical of the displacements caused by the packing defects in FCC crystals. The above-mentioned effects support the assumption on the presence of numerous packing defects in the diamond films. In this connection, the average coherence length L in the diamond films was calculated from the Selyakov-Scherer equation using the narrowest and most intense (220) reflection. At the 1.7 μm film thickness, the crystallite size is 30 nm; as the film thickness increases to 9 μm, this grows slightly, then being stabilized at 40 nm.

An important feature of the films on the substrates is the residual stress level. X-ray tensometric determination of the stress in the coatings was carried out by $\sin^2\psi$ method using multiple oblique scans of the (331) reflection positioned in the 2θ diffraction angle range near 141 degrees. Even for the scanning with focusing ($\psi = 0$), the diffraction lines were found to be very broad (1.5 to 2 degrees), thus additionally confirming the high film defectness. Due to both low intensity and large width of the reflections, it was impossible to determine

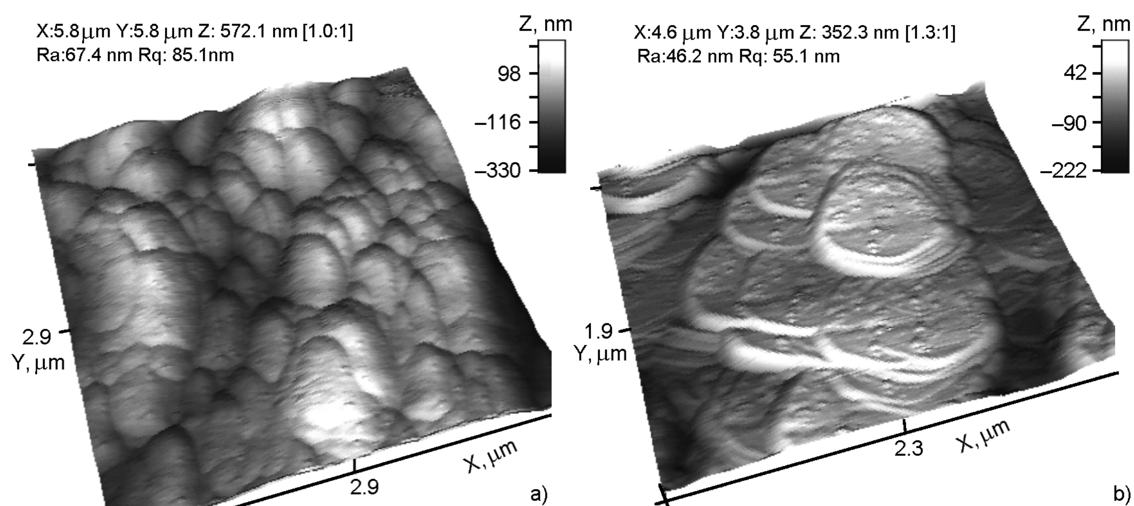

Fig. 4. Surface morphology of diamond films on silicon surfaces untreated (a) and polished (b) prior to UDD sowing.

the stress degree in the films with thickness less than 5 μm, however, these measurements have been carried out for 9.7 μm and 11.7 μm thick films. The d–$\sin^2\psi$ plots obtained for these samples after the diffraction pattern treatment are shown in Fig. 3. The experimental points fall well onto the straight lines, the slope thereof indicating the diamond films are compressed. Using the technique described in detail in [6], the residual stresses were calculated from the d–$\sin^2\psi$ plots, and the diamond film crystal lattice period corresponding to non-stressed state was obtained. The stress value in the film of 9.7 μm is −0.3 GPa, that corresponds to the lower limit of stress registration for X-ray tensometric method. In the 11.7 μm film, the stress is higher and reaches −0.7 GPa. Such the stress level variation in the diamond films of different thickness seems to be due to the different relaxation extent of thermal compressive stress, σ_t, caused by different thermal expansion coefficients of the coating and the substrate when the deposition takes place at a high temperature. The σ_t calculations described in [11] give ~ 3 GPa compressive stresses that is substantially higher than our experimental values. Perhaps the stress relaxation is easier in the thinner film than in the thicker.

The crystal lattice parameter was found to be somewhat lower than the reference value for the natural diamond (a = 0.3567 nm) and was 0.3563 nm for the film of 9.7 μm, and 0.3565 nm for 11.7 μm film. Such lowering may be due to different causes. In the present case, the most substantial factor seems to consist in the influence of packing defects mentioned above. The existence of the packing defects results in the diamond (331) diffraction line displacement to larger angles, which results in decrease of the lattice parameter. The higher is the defect concentration in the thin film, the stronger this effect is.

It is to note that the diamond films prepared in multi-component $CH_4/H_2/Ar$ gas mixture differ considerably from the films deposited in the CH_4/H_2 mixture, studied before and being non-textured diamond films with the lattice parameter close to the reference value and relatively low content of the defects such as dislocations and dislocation walls [2–4]. Thus, the working gas content change stimulates the texture formation and increases the defect concentration in the diamond films. At that, the surface morphology is changed cardinally. Introduction of argon into the gas mixture results in loss of the morphology stability of the facet type growth: the films with distinct facets and block structure are transformed into nano-crystalline ones [7, 8].

In Fig. 4–6, the atomic force microscopic images of the diamond coatings synthesized in the $CH_4/H_2/Ar$ mixture are presented at various magnifications. The coating microstructure appears as intergrown round section clusters of sizes exceeding one μm with surface coated with smaller nano-sized formations. A similar structure, the so-called "cauliflower", was observed for nano-crystalline coatings described in [12]. Depending on the technique of the silicon substrate

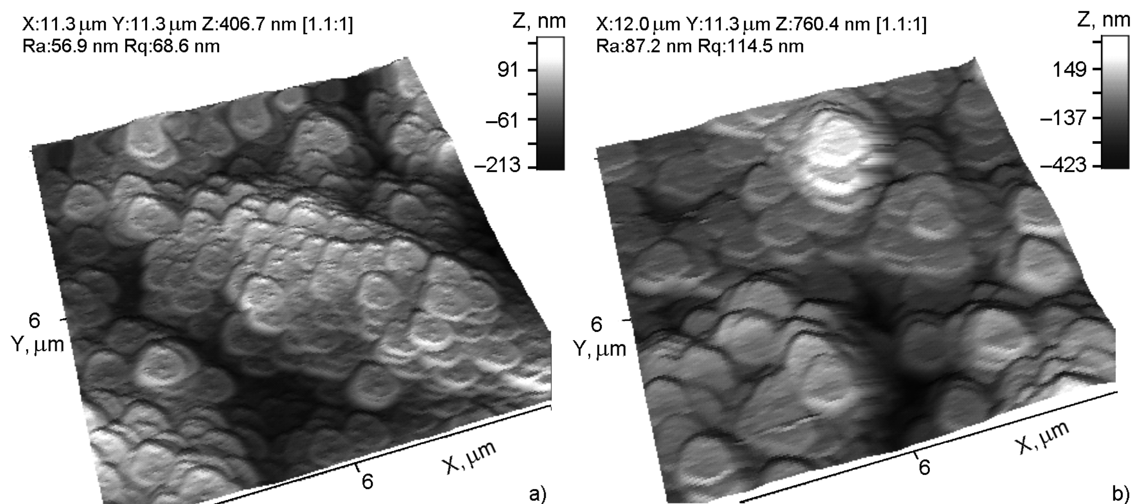

Fig. 5. Surface morphology of 1.7 µm (a) and 7.8 µm (b) thick diamond films.

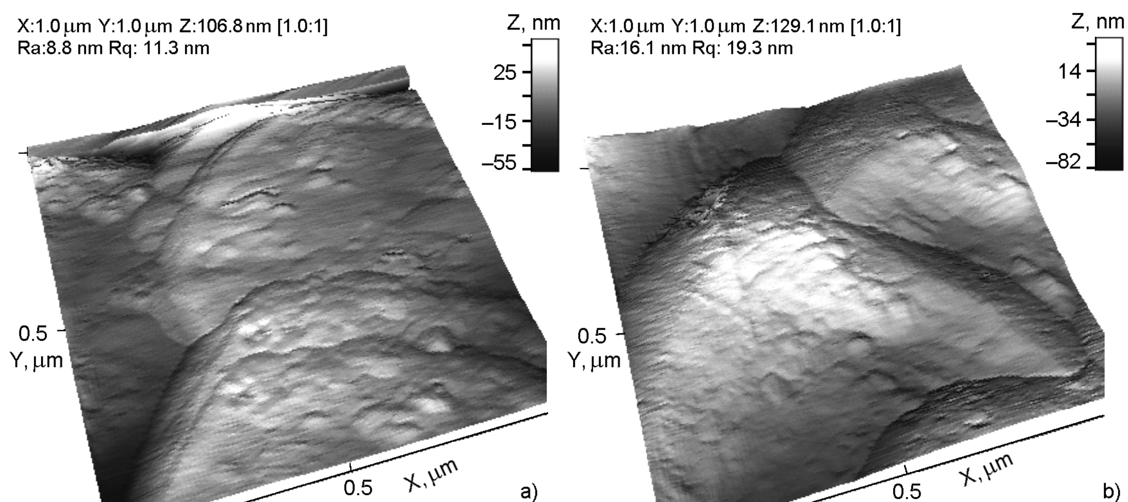

Fig. 6. Growth surface structure of 1.7 µm (a) and 7.8 µm (b) thick diamond films.

preliminary preparation, the micrometer size clusters are either strongly convex (Fig. 4a) or flat enough (Fig. 4b). The convex formations grow on the substrates not polished prior to UDD "sowing". The similar surface morphology is also typical of the films deposited on molybdenum substrates [8]. The flatter formations are observed in the films deposited onto silicon substrates polished prior to the UDD sowing using abrasive sandpaper and diamond paste.

No substantial morphology differences have been revealed in the films of different thickness (Fig. 5, 6). This concerns the films deposited onto both the polished and unpolished substrates. Noteworth is only the difference between the microstructure elements, which diameter increases almost twice as the film thickness grows from 1.7 to 4.6 µm. However, a further thickness increase does not result in any significant changes (Fig. 5a and 5b). For all the films studied, the average surface roughness R_a does not exceed 100 nm. As to the nanostructure element size, those have no substantial differences for the films of different thickness (Fig. 6a and 6b), that indicates the stability of the nano-structure formation process. The cluster surface microroughness R_a is 10 to 20 nm for all the films. The profilogram analysis shows that the structure formations atn the micro-cluster surface have diameters in the range of 20 to 60 nm. The average values are close to the coherence lengths L determined by X-ray diffraction method, this suggests to consider the L value as the diamond nanograin average size in the films.

The "cauliflower" structure formation can be explained by the growth of diamond primary nuclei indented into the substrate by "sowing", and the simultaneous rapid formation of secondary nuclei at the growth surface. As a result, the film consists of agglomerates consisting of diamond nanocrystals. The increase of the agglomerate size continues until they encounter other similar formations, as in the case of the island film growth. Indeed, the microstructure formation size is about 1 μm, corresponding to island sizes to the instant of their coalescence into a continuous film at the nucleation density about ~ 10^8 cm^{-2} at the substrate surface. As the film thickness grows, a fraction of the conglomerates are associated forming larger clusters. The size of cluster forming nano-crystallites is practically unchanged and defined by the deposition parameters.

The mechanism described above allows to explain not only the peculiarities of the coating morphology, but also the origin of the texture formation in the films. In [13], the texture formation is supposed to be caused by oriented nucleation and growth of secondary nano-crystals at the surface of the growing clusters. As a result, the micrometer size clusters shaped as hemispheres are formed by the diamond nanocrystals with <110> direction oriented along the sphere radius. The thicker the film and larger the cluster radius, the larger is the part of nano-crystals oriented with <110> direction near the normal to film surface, and more intense are the (220) lines on the diffraction patterns. Our experimental results on the deposition of nano-crystalline diamond films in the glow discharge agree well with the growth model suggested.

The authors are very thankful to the coworkers of the Laboratory of Analytical Optochemotronic headed by Prof.N.N.Rozhitskiy at Kharkiv National University of Radioelectronics for the measurements using atomic-force microscope.

References

1. A.I.Gusev, Nano-materials, Nano-structures, Nano-technologies, "FISMATLIT", Moscow (2005) [in Russian].
2. H.Gleiter, *Acta Mater.*, **48**, 1 (2000).
3. D.M.Gruen, *Annu. Rev. Mater. Sci.*, **29**, 211 (1999).
4. V.K.Pashnev, O.A.Opalev, V.I.Gritsyna et al., *Fizich. Inzhener. Poverkhnost'*, **1**, 49 (2003).
5. I.I.Vyrovets, V.I.Gritsyna, O.A.Opalev et al., *Fizich. Inzhener. Poverkhnost'*, **5**, 87 (2007).
6. I.I.Vyrovets, V.I.Gritsyna, S.F.Dudnik et al., *VANT, Ser:Vacuum, Chist/Mater., Sverkhprovodn. (2008), No.1, p.142.*
7. I.I.Vyrovets, V.I.Gritsyna, S.F.Dudnik et al., in: Proc. of Kharkiv Nano-technology Assembly, Kharkiv, Ukraine (2008), v.1, p.248.
8. I.I.Vyrovets, V.I.Gritsyna, S.F.Dudnik et al., in: Proc. of 21 Int. Symp."Thin Films in Electronics" OAO "ZNITI TEHNOMASH" Publ. Moscow (2008), p.377.
9. S.S.Gorelik, Yu.A.Skakov, L.N.Rastorguyev, X-ray and Electron-Optical Analysis, MISIS Publ., Moscow (1994) [in Russian].
10. Ya.S.Umanskiy, X-ray Analysis of Metals, Metallurgia, Moscow (1967) [in Russian].
11. A.Heiman, E.Lakin, E.Zolotoyabko, A.Hoffman, *Diamond & Related Mater.*, **11**, 601 (2002).
12. Y.K.Liu, P.L.Tso, I.N.Lin et al., *Diamond & Related Mater.*, **15**, 234 (2006).
13. F.Silva, F.Benedic, P.Bruno, A.Gicquel, *Diamond & Related Mater.*, **14**, 398 (2005).

Морфологія поверхні та структура нанокристалічних алмазних плівок, отриманих у $CH_4/H_2/Ar$ плазмі тліючого розряду

І.І.Вировець, В.І.Грицина, С.Ф.Дуднік, О.А.Опалєв, О.М.Решетняк, В.Є.Стрельницький

Алмазні плівки товщиною до 12 мкм отримано на підкладках з монокристалічного кремнію методом газофазного осадження у $CH_4/H_2/Ar$ плазмі тліючого розряду, стабілізованого магнітним полем. Методами рентгеноструктурного аналізу та атомно-силової мікроскопії встановлено, що плівки складаються з конгломератів діаметром ~ 1 мкм, утворених нанокристалами алмазу із середнім розміром 30–40 нм. З ростом товщини плівки від 1,7 до 11,7 мкм розмір конгломератів збільшується у 2 рази. При цьому розмір нанокристалів практично не змінюється. У плівках виявлено текстуру, залишкові напруження стиску та високий вміст дефектів кристалічної структури.